

# Numerical simulation of the structural behaviour of threaded anchors in UHPFRC

**Antonina Hochuli** (corresponding author), Doctoral student, Laboratory for Maintenance and Safety of Structures, Swiss Federal Institute of Technology (EPFL), Lausanne, Switzerland,  
Email: [antonina.hochuli@epfl.ch](mailto:antonina.hochuli@epfl.ch)

**Eugen Brühwiler**, Full Professor, Laboratory for Maintenance and Safety of Structures, Swiss Federal Institute of Technology (EPFL), Lausanne, Switzerland,  
Email: [eugen.bruehwiler@epfl.ch](mailto:eugen.bruehwiler@epfl.ch)

## Abstract

Thanks to the relatively high tensile strength and very dense matrix, UHPFRC has established itself as an excellent building material for strengthening existing highly stressed structures as well as for the construction of new structures. In both cases, the use of fasteners is unavoidable. Often, threaded anchors are used as fasteners. The thicknesses of structural components made of UHPFRC are relatively thin, i.e., at least 30mm (1.18 in), typically 50 to 100mm (1.97 to 3.94 in) and exceptionally 100 to 200mm (3.94 to 7.87 in). Therefore, the aim is to use fasteners with short anchorage lengths in order to anchor them safely in UHPFRC.

In this contribution, the structural behaviour of a short, threaded anchor with a diameter of 20 mm (0.79 in) and an embedment length in UHPFRC of 50 mm (1.97 in) ( $2.5\phi$ ) was investigated by means of numerical simulations using a non-linear Finite Element model. UHPFRC was assumed to show tensile strain hardening behaviour and a tensile strength of 7 MPa (1.02 ksi) and 11 MPa (1.6 ksi), respectively. The investigated element was subjected to a continuously increasing uniaxial pull-out force. The results reveal the fracture mechanism of threaded anchors in UHPFRC being characterized by the formation of a UHPFRC tensile membrane as the main resistance against the pull-out force. Also, the influence of the tensile properties of UHPFRC on the pull-out behavior and ultimate resistance of threaded anchors in UHPFRC is determined.

**Keywords:** short anchorage, threaded anchor, numerical simulation, structural behavior

## 1. Introduction

The use of Ultra-High Performance Fibre Reinforced Cementitious Composites (UHPFRC) has increased significantly in recent years. This new building material has established itself as an effective material for the rehabilitation and strengthening of existing structures as well construction of new structures such as bridges and highly stressed structural members. One recent application was in the domain of fixed railway tracks (A Hochuli, E. Brühwiler, J.-G. Trouillet 2022). Due to its relatively high tensile, compressive and fatigue strengths as well the deformation capacity compared to concrete, UHPFRC has the potential to provide economically and technically more effective engineering solutions.

Since, the structural components made of UHPFRC show a thickness of at least 30mm (1.18 in) and typically 50 to 100mm (1.97 to 3.94 in) and, exceptionally, 100 to 200mm (3.94 to 7.87 in), fasteners like threaded anchors are used with relatively small embedment lengths. However, current anchor systems, which are available on the market, were initially developed for concrete and, therefore, presuppose a relatively long embedment length, usually at least 8 cm (3.15 in), which allows anchoring under the upper reinforcement layer.

In the following, this contribution presents the results of a numerical investigation of the load-bearing behavior of UHPFRC subjected to quasi-static pull-out force, which is applied to a short, threaded anchor fixed in the UHPFRC layer.

## 2. Numerical simulation

### 2.1. Purpose of the numerical simulation

A finite element simulation is an approach that does not require material resourcing and laboratory equipment but enables an investigation of load-bearing behaviour, providing important information. This approach is used in the current research and can be further used as an effective means in planning laboratory tests. Since no comparable laboratory tests have been performed before, the properties of simulated building material were validated by means of simulations of 4-point bending tests for each UHPFRC mix and comparison of numerical and experimental results.

### 2.2. Setup of the numerical model

The numerical model represents a cubic volume element, according to Figure 1 (a) ①, which is conceptually cut out from a large composite slab of UHPFRC and concrete. A cast-in-place short threaded anchor of 20 mm (0.79 in) diameter ② with an embedment length of 50 mm (1.97 in) and 6 force-transmitting 5 mm (0.20 in) wide flanks is fixed in the UHPFRC layer. The cubic volume element consists of two model-relevant macro-elements according to Figure 1 (b) with two types of mesh and finite elements size, which are monolithically connected. The lateral and vertical surface supports ③ ④ assigned to the edges induce no compression on the cubic volume element. The support reaction on these element edges is controlled during the loading process. The maximum and minimum support forces are given by the tensile and compressive strength of UHPFRC and the displacement.

### 2.3. Simulation of building material

The numerical simulation is performed using the FE program ATENA (Vladimír Červenka 2021). The UHPFRC was assumed to be homogeneous and modelled using *Cementitious2 UserHCC* numerical material with the strain-hardening and -softening domain according to Table 1. The model for degradation of tensile properties is based on the smeared crack model (Zdenek P. Bazant 1983).

In addition, the finite element size  $L_t$  of 3 mm (0.12 in) was iteratively chosen for the macro elements, which represent the anchor and the UHPFRC around the anchor since the anchor flanks are only 5 mm wide. The definition of the value  $L_t$  which relevant for the characteristic crack bandwidth (J. Cervenka 2018), is showed schematically in Figure 1 (b).

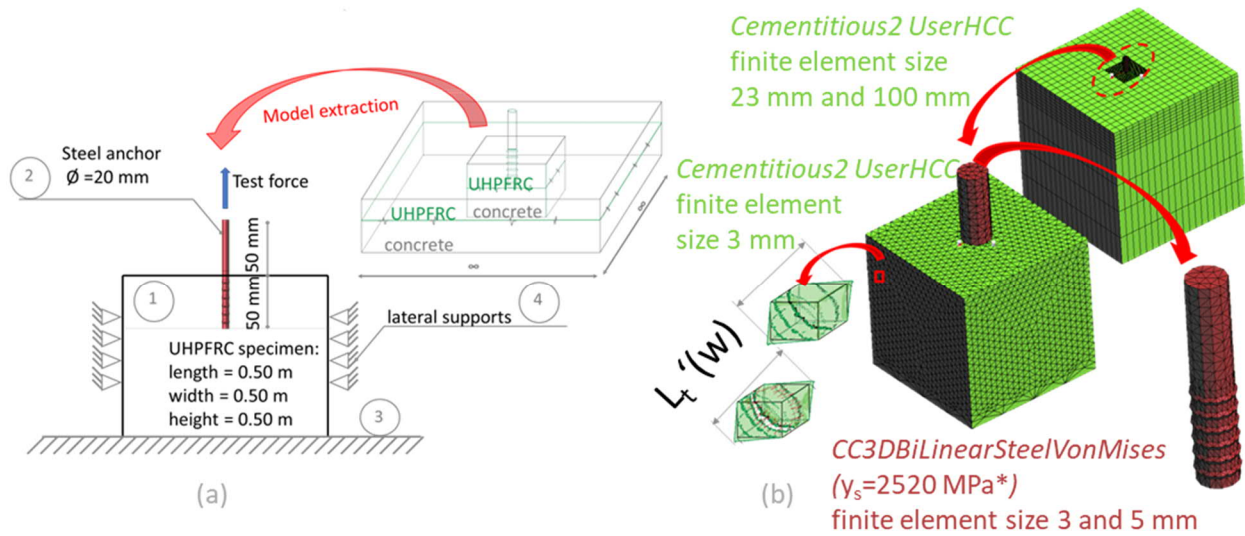


Figure 1 (a) Schematic presentation of the experimental installation, (b) FE-model.

Table 1 UHPFRC-mixes for quasi-static tests

		Tensile strength of UHPFRC	
		UHPFRC 11	UHPFRC 7
Tensile strength	$f_{Utu}$	11.5 MPa (1.67 ksi)	7.1MPa (1.03 ksi)
Elastic limit	$f_{Ute}$	9.8 MPa (1.42 ksi)	6.9 MPa (1 ksi)
Strain in UHPFRC at tensile strength	$\epsilon_{Utu}$	2.29‰ (0.00229)	1.5 ‰ (0.0015)
Strain in UHPFRC at elastic limit stress	$\epsilon_{Ute}$	0.22‰ (0.00022)	0.15 ‰ (0.00015)
Fiber length	$l_f$	14mm (0.55 in)	13 mm (0.51 in)
Fiber diameter	$d_f$	0.16mm ( $6 \cdot 10^{-3}$ in)	0.16mm ( $6 \cdot 10^{-3}$ in)

### 2.4. Modelling of the quasi-static loading

The quasi-static pull-out force is modelled as gradually increasing uniaxial force of 5kN (1.12 kip) in the anchor per loading step at the top of the anchor.

### 3. Results

The finite element models were loaded until the loss of stability of the static system occurred, in other words, to the change of state of the system from static to kinematic, which took place shortly after reaching the ultimate force  $F_u$ . Since a real process would be run until the real crack of width  $w=l_f/2$  occurs, the obtained force-displacement curve was supplemented with the dashed decreasing branch.

Figure 2 (a) presents the obtained force-displacement curves for UHPFRC 11 and UHPFRC 7. On the vertical axis, the introduced pull-out force is showed, which is calculated from the recorded strain of the anchor material at the level of the UHPFRC surface (Point O Figure 2 (b)). The vertical

displacement  $\delta$  respectively  $\Delta l$  (Figure 2 (b) that is recorded directly during the numerical simulation is showed on the horizontal axis. As can be seen in Figure 2 (a), the ultimate force  $F_u$  was achieved at 25-30% of the maximum vertical displacement. Moreover, it was found that the increasing branch consists of 3 parts with different slopes, which correspond to 3 stages of the fracture process showed in Figure 2 (a) on the right of the diagram.

Hence, for detailed analysis of the results, the entire loading process is divided into 3 loading phases (L. Ph.) according to 3 stages of the fracture process as follows: L. Ph I: loading up to 30%  $F_u$ , L. Ph II: loading up to 75%  $F_u$ , L. Ph III: loading up to 100%  $F_u$ .

Since this work is based on numerical simulation, the advantage of this approach can be used in directly analysing the strain fields in the middle cross-section.

### 3.1. Global fracture process

Figure 3 and Figure 4 show the plots of maximum principal strain during the entire loading process. These plots are supplemented with red and blue arrows, which help to follow the propagation of the fracture process. The red arrows highlight the tensile strain propagation in the radial direction, and the blue arrows show the spreading of the compression field (compressive strain), which was extracted from the plots of minimal principal strain.

In the loading phase I, which lasts from the 0 kN to 30%  $F_u$ , the fracture process starts to propagate in the upper area of the UHPFRC-layer around the threaded anchor as an approximately 5 mm (0.2 in) thin horizontal circular tensile field ( $\epsilon_{rad}$ ) and an inclined field ( $\epsilon_{cone}$ ) perpendicular to the UHPFRC-cone, which can be observed on the plot for the loading with  $F=12.14$  kN (2.73 kip).

The analysis of the strain fields reveals that the introduced pull-out force via the threaded anchor in UHPFRC first causes the conical compression ( $-\epsilon$ ) and the horizontal circular tension fields ( $\epsilon_{rad}$ ) in the UHPFRC layer. As long as the compression ( $\sigma_{compression} \leq f_{Uc}$ ) and the tension ( $\sigma_{tension} \leq f_{Ut}$ ) stresses are transmitted in the UHPFRC, the anchorage is ensured. Thereby, the UHPFRC behaves in the stain-softening domain directly around the threaded anchor, already at  $F=10-15\%$   $F_u$ .

The inclined tensile field ( $\epsilon_{cone}$ ) occurs as a result of the pulling out of the entire region, which contains the threaded anchor and the UHPFRC-cone that includes the circular horizontal tension ( $\epsilon_{rad}$ ) and the conical compression ( $-\epsilon$ ) fields.

During the loading phase II, which lasts until 75%  $F_u$ , the horizontal circular tensile field ( $\epsilon_{rad}$ ) increases further and comprises the UHPFRC-cone at the end completely, as can be seen on the plots of the principal strains.

Moreover, with increasing the circular tension field ( $\epsilon_{rad}$ ), the height of the UHPFRC-cone decreases. And at the end of the loading phase II, the fracture mechanism consists only of the circular tension field of the thickness that is equal to the embedment length of the threaded anchor  $l_{embedment}$ . From a static viewpoint, the circular tension field ( $\epsilon_{rad}$ ) behaves as a tensile membrane.

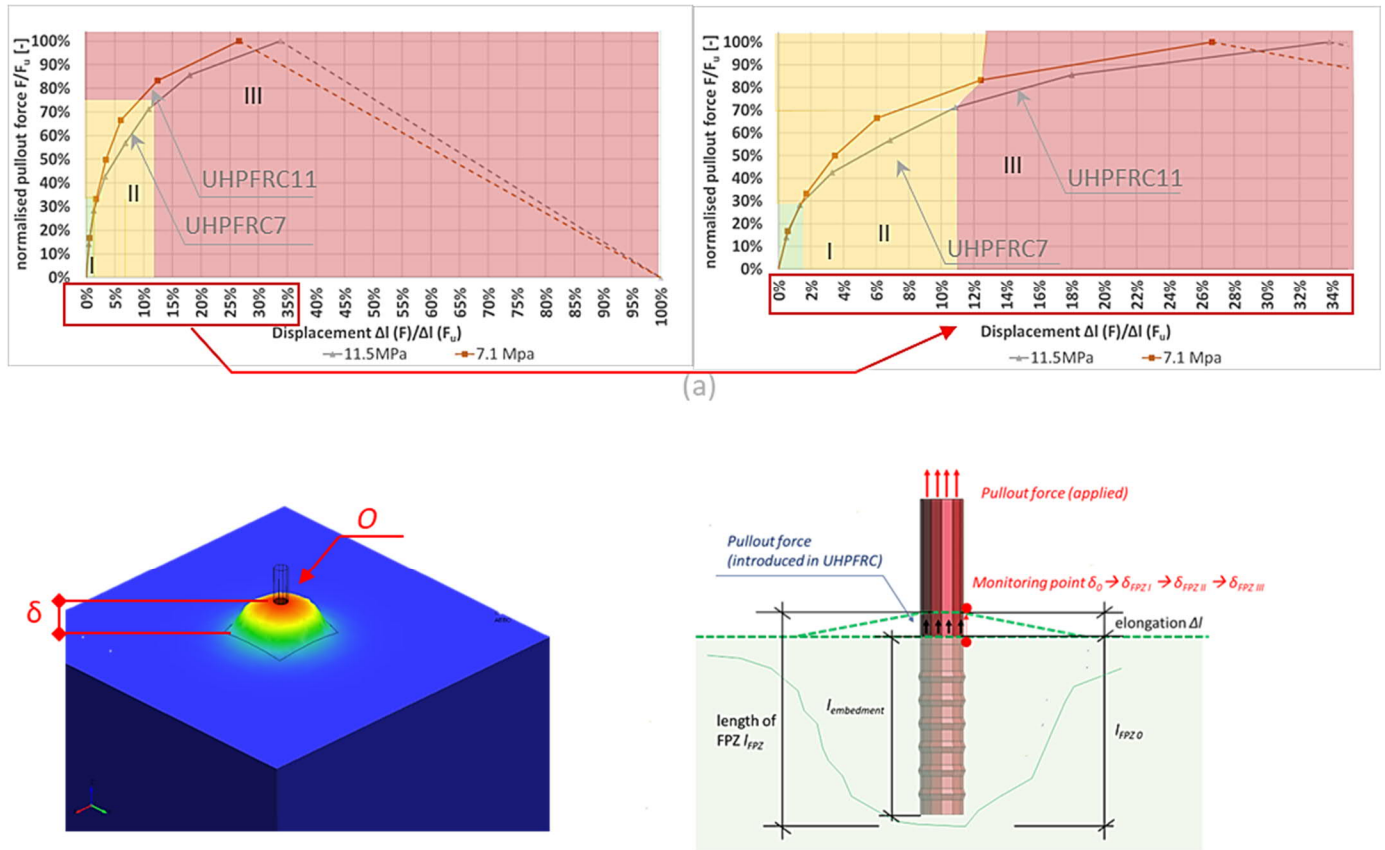


Figure 2 Pull-out force-displacement diagram for the threaded anchor  $\varnothing 20$  mm (0.79 in)  $l_{\text{embedment}} = 50$  mm (1.97 in)

The loading phase III begins with the fully formed tensile membrane of the thickness  $l_{\text{membrane}} \approx 1.0-1.1 l_{\text{embedment}}$  as a main resistance against the pull-out force applied to the threaded anchor, which is located in the middle of this tensile membrane. Since, the pull-out force leads to compression on the contact surfaces between anchor flanks and UHPFRC, the inclined conical compression field ( $-\varepsilon$ ) is observed also within the tensile membrane and causes further increasing tensile stain in the upper third of the tensile membrane.

### 3.2. Fracture process within the UHPFRC tensile membrane

Due to tensile properties and the deformation capacity of UHPFRC, a horizontal circular tension field forms around the anchor subjected to the pull-out force. This tension field behaves as a tensile membrane. The outer part of the tensile membrane, which corresponds to approx. 60% of the membrane radius remains in the elastic domain, while the membrane radius itself and the membrane increase under the continuously increasing pull-out force. Thus, the fracture process zone is localised in the inner part of the tensile membrane, which corresponds to 40% of the membrane radius. In the radial direction, the tensile membrane extension increases up to 5 times faster than in the vertical direction. At approximately 75% of the ultimate force  $F_u$ , the tensile membrane is fully formed with the thickness that corresponds to the embedment length of the threaded anchor  $l_{\text{embedment}}$  and the radius of approximately  $5 l_{\text{embedment}}$ .

The force introduction in the fully formed tensile membrane takes place via compression on the contact surface between the anchor flanks and UHPFRC, which leads to the increase of tension in the upper third of the tensile membrane.

In the end, the anchorage failure occurs due to the local extension of the tensile membrane around the anchor and the pulling out of the threaded anchor from UHPFRC body.

Summarised, it results from this study that only two fracture modes for short, threaded anchors in UHPFRC are possible:

1.  $F_{u \text{ anchor}} < F_{u \text{ membrane}}$ : fracture of anchor material
2.  $F_{u \text{ anchor}} > F_{u \text{ membrane}}$ : pulling anchor out from the UHPFRC, due to local fracture of the tensile membrane within  $0.35 R_{\text{membrane}}$

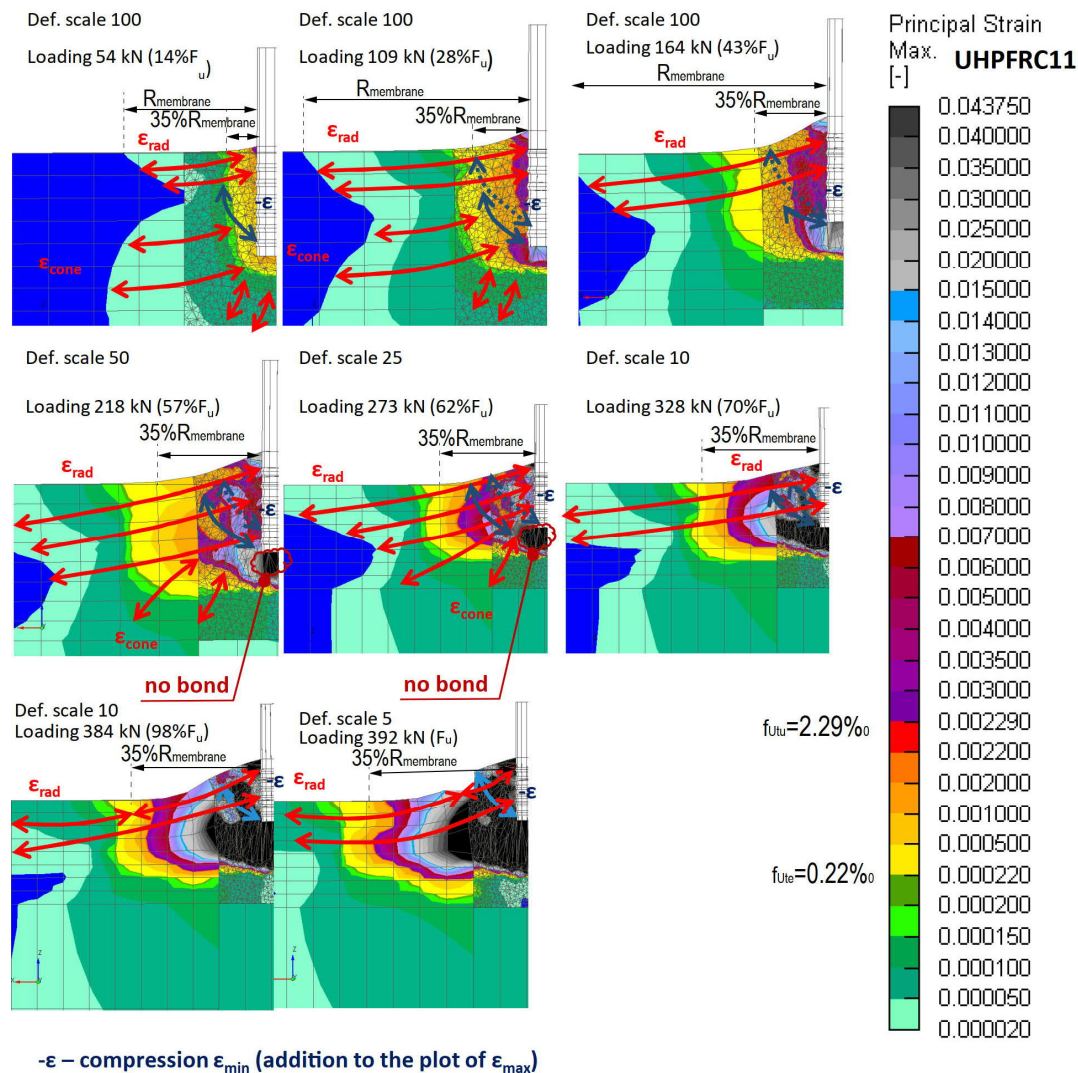


Figure 3 Development of the membrane in the UHPFRC 11 (Output ATENA principal strain max).



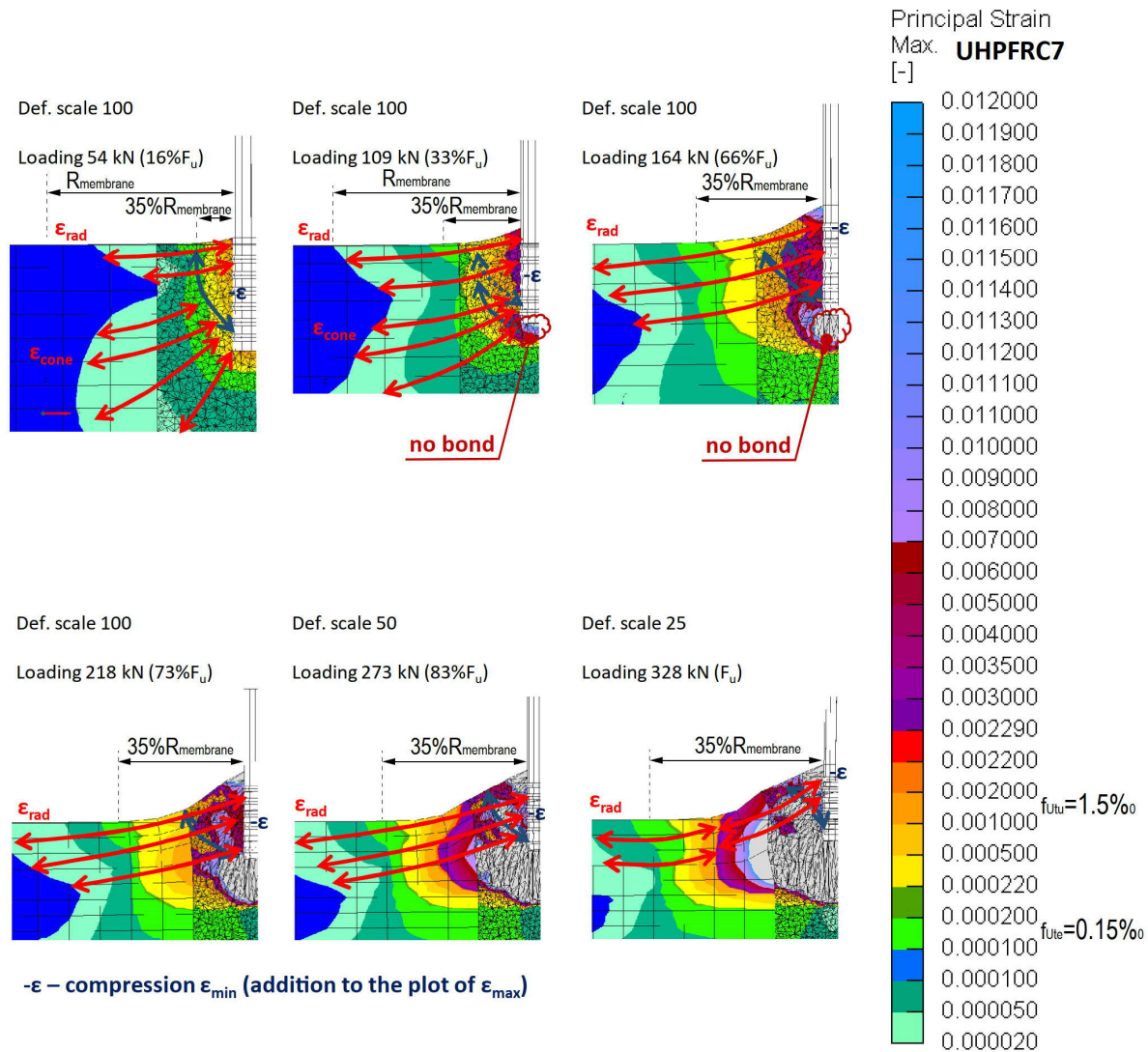


Figure 4 Development of the membrane in the UHPFRC 7 (Output ATENA principal strain max)

#### 4. Conclusion

This investigation has revealed that the UHPFRC subjected to pull-out force behaves quite differently from today's known cementitious building materials like concrete. Due to its tensile strength, the introduced tension is transmitted in the tensile fields. With sufficient structural element size (the distance from the anchor to the structural element edge should be approximately five times greater than the embedment length of the anchor), the tensile membrane expands in horizontal and vertical directions. In this study, it was found that the maximum extension of the membrane in the horizontal radial direction is approximately 5 times the membrane thickness.

## **5. Literature**

- A Hochuli, E. Brühwiler, J.-G. Trouillet. „Improvement of fixed railway tracks using fatigue-resistant cementitious fibre reinforced composite material“, Montpellier, France, 2022. [www.railwaysconference.com](http://www.railwaysconference.com)
- J. Cervenka, V Cervenka, S. Laserna. „On crack band model in finite element analysis of concrete fracture in engineering practice“, Engineering Fracture Mechanics 2018: 27-47. [www.elsevier.com/locate/engfracmech](http://www.elsevier.com/locate/engfracmech)
- R. Pukl, D. Novák, T. Sajdlová, D. Lehký, J. Červenka, V. Červenka. “Probabilistic design of fibre concrete structures” IOP Conference Series: Materials Science and Engineering. Prague, Czech Republic: IOP Publishing Ltd, 2017. <https://iopscience.iop.org/article/10.1088/1757-899X/246/1/012004>
- Rolf Eligehausen, Roland A. Cook, Jörg Appl. „Behavior and Design of Adhesive Bonded Anchors“, Bd. 103. 6. Hrsg. Structural Journal. American concrete Insitute, aci, 1. 11 2006. 882-832. <https://www.concrete.org/publications/internationalconcreteabstractsportal.aspx?m=details&ID=18234>
- Vladimír Červenka, Libor Jendele, Jan Červenka. ATENA Program Documentation Part 1, Theory. Prague, 2021.
- Zdenek P. Bazant, B.H. Oh. “Crack band theory for fracture of concrete.” RILEM 1983.